

Spatial heterogeneity of tundra vegetation response to recent temperature changes

GENSUO J. JIA*†, HOWARD E. EPSTEIN† and DONALD A. WALKER‡

*RCE-TEA, Institute of Atmospheric Physics, Chinese Academy of Sciences, PO Box 9804, Beijing 100029, China,

†Department of Environmental Sciences, University of Virginia, Charlottesville, VA 22904, USA, ‡Institute of Arctic Biology, University of Alaska Fairbanks, Fairbanks, AK 99775, USA

Abstract

The spatial heterogeneity of recent decadal dynamics in vegetation greenness and biomass in response to changes in summer warmth index (SWI) was investigated along spatial gradients on the Arctic Slope of Alaska. Image spatial analysis was used to examine the spatial pattern of greenness dynamics from 1991 to 2000 as indicated by variations of the maximum normalized difference vegetation index (Peak NDVI) and time-integrated NDVI (TI-NDVI) along latitudinal gradients. Spatial gradients for both the means and temporal variances of the NDVI indices for 0.1° latitude intervals crossing three bioclimate subzones were analyzed along two north–south Arctic transects. NDVI indices were generally highly variable over the decade, with great heterogeneity across the transects. The greatest variance in TI-NDVI was found in low shrub vegetation to the south (68.7–68.8°N) and corresponded to high fractional cover of shrub tundra and moist acidic tundra (MAT), while the greatest variance in Peak-NDVI predominately occurred in areas dominated by wet tundra (WT) and moist nonacidic tundra (MNT). Relatively high NDVI temporal variances were also related to specific transitional areas between dominant vegetation types. The regional temporal variances of NDVI from 1991 to 2000 were largely driven by meso-scale climate dynamics. The spatial heterogeneity of the NDVI variance was mostly explained by the fractional land cover composition, different responses of each vegetation type to climate change, and patterned ground features. Aboveground plant biomass exhibited similar spatial heterogeneity as TI-NDVI; however, spatial patterns are slightly different from NDVI because of their nonlinear relationship.

Keywords: Alaska, Arctic, biomass, climate change, fractional cover, heterogeneity, NDVI, transects, tundra, variability

Received 30 April 2004; revised version received 28 January 2005, 08 April 2005; accepted 22 August 2005

Introduction

Arctic tundra ecosystems are warmth-limited and can respond to temperature dynamics on a relatively short time scale (Hobbie & Chapin, 1998; Arft *et al.*, 1999; Chapin *et al.*, 2000). Therefore, they are expected to be highly sensitive to both environmental fluctuation and directional climate change and to play a significant role in biospheric feedbacks to global climate (Bonan *et al.*, 1995; Anisimov *et al.*, 1997; Levis *et al.*, 1999; Chapin

et al., 2005). Indeed, tundra ecosystems have changed substantially in terms of primary production, shrub abundance, and carbon exchange (Chapin *et al.*, 1995; Oechel *et al.*, 2000; Sturm *et al.*, 2001; Walker *et al.*, 2004) as warming of Alaska and other parts of the Arctic has accelerated over the past three decades (Serreze *et al.*, 2000; Moritz *et al.*, 2002). Changes in arctic landscapes are relevant across the entire circumpolar region, a general trend of increase in vegetation greenness in response to rising air temperature (Zhou *et al.*, 2001; Lucht *et al.*, 2002) and a short-term decrease following the Mt. Pinatubo eruption (Lucht *et al.*, 2002; Hope *et al.*, 2003) have been detected throughout northern latitudes over the 1990s. However, the magnitude of changes in vegetation greenness was not likely homogenous across

Correspondence: Gensuo Jia, Department of Environmental Sciences, University of Virginia, Charlottesville, VA 22904, USA.
tel. +1 434 9822337, fax +1 434 9822137,
e-mail: jiongjia@cnr.colostate.edu

landscapes and regions. Remotely sensed studies (Zhou *et al.*, 2001), site-scale field measurements (Hobbie & Chapin, 1998; Arft *et al.*, 1999; Walker *et al.*, 2004) and simulation modeling (Epstein *et al.*, 2000, 2004b) all suggest spatially heterogeneous response of vegetation greenness to global climate change. In this paper, we integrate long-term remotely sensed data analyses and field measurements to investigate the spatial patterns of vegetation dynamics in response to climate fluctuation along bioclimate and latitudinal gradients in northern Alaska.

The normalized difference vegetation index (NDVI), and its features of daily repeating and large spatial coverage as derived from NOAA's Advanced Very High-Resolution Radiometer (AVHRR) sensors, is a useful indicator for monitoring spatial heterogeneity of temporal changes in vegetation across large and remote regions, such as the Arctic of northern Alaska.

In this study, we analyzed the interannual patterns of maximum NDVI (Peak-NDVI) and temporally integrated NDVI (TI-NDVI) across latitudinal gradients and bioclimate subzones (Walker, 2000) in the Arctic of Alaska, using AVHRR-NDVI derived from a 10 year (1991–2000) biweekly time series of 1 km² resolution data. We were interested in analyzing the spatial heterogeneity of decadal changes of vegetation greenness and identifying the most sensitive locations with the highest temporal variability, in addition to investigating potential driving forces behind the temporal NDVI variances and their spatial heterogeneity. NDVI, as an indicator of photosynthetic activity, should vary with summer warmth in these warmth-limited ecosystems of the Arctic, and NDVI variance should reflect the dynamics of productivity of dominant vegetation types that are likely to respond to climate change in different ways.

Materials and methods

Study site

The study was conducted on the Arctic Slope of Alaska, the northernmost part of the state, which lies entirely above the Arctic Circle (Fig. 1). The region is dominated by various tundra vegetation types within three bioclimate subzones: prostrate dwarf shrub subzone (subzone C), erect dwarf shrub subzone (subzone D), and low shrub subzone (subzone E) (Walker, 2000) (Table 1). Vegetation is highly heterogeneous, with a spatial pattern that generally follows gradients of latitude and summer air temperature (from the coast inland), and is affected by the highly heterogeneous soil parent materials and the existence of thaw lakes, frost boils and other patterned ground features (Walker *et al.*, 1998).

Two latitudinal transects within the Arctic Slope, with geographic extents of 68.2–71.4°N for the western transect and 68.4–70.6°N for the eastern transect were selected as the areas for intensive field and temporal-spatial modeling studies to examine the heterogeneity of vegetation dynamics across the three bioclimate subzones. Sites along these transects have been used as experimental and observational areas by the Land Atmosphere Ice Interaction (LAI) program (LAI, 1997), the International Tundra Experiment (ITEX) (Arft *et al.*, 1999), the Circumpolar Active Layer Monitoring (CALM) program (Brown *et al.*, 2000), and most recently by an NSF arctic biocomplexity study (Walker *et al.*, 2004). Many studies of spatial patterns and temporal dynamics of tundra vegetation, including field measurements, warming chamber experiments and modeling have been and continue to be focused at sites within these transects (e.g. Hobbie & Chapin, 1998; Oberbauer *et al.*, 1998; Walker *et al.*, 1998, 2003a, b; Epstein *et al.*, 2000, 2004a, b; Oechel *et al.*, 2000; Walker, 2000; Jia *et al.*, 2002, 2003).

NDVI indices

AVHRR-derived 1 km biweekly composited NDVI time series from 1991 to 2000 acquired by the US Geological Survey (USGS) Biological Resources Division were used as basic data sets to investigate spatial and temporal patterns of various NDVI indices in the study areas. The NDVI is an index of vegetation greenness calculated from spectral reflectance in red (ρ_{red} , 0.58–0.68 μm) and near infrared (ρ_{nir} , 0.725–1.1 μm) bands ($\text{NDVI} = (\rho_{\text{nir}} - \rho_{\text{red}}) / (\rho_{\text{nir}} + \rho_{\text{red}})$) (Goward *et al.*, 1991). Maximum value compositing (MVC) on daily data was used to compose NDVI biweekly data sets to reduce atmospheric effects and cloud contamination that commonly existed in AVHRR daily data sets (Gutman, 1991). The biweekly composited NDVI datasets were received in band sequential (BSQ) image format and image processing software (ArcInfo, ESRI, Redland, CA, USA) was used to convert the images into raster grid format and to extract the portion of our study areas. Additional geo-referencing was performed for selected periods with high registration errors, using USGS Alaska boundary coverage, Alaska river coverage, and a digital elevation model at the same spatial resolution.

Data for this study were recorded by AVHRR sensors onboard NOAA-11 and NOAA-14 satellites from 1991 to 2000. NOAA-11 data were used for the 1991–1994 data sets, while NOAA-14 data were used for the 1995–2000 data sets. The composite period also varied between the early and late 1990s. The 1991–1994 data sets are based on a bimonthly (15 or 16 days) composite period. The 1995–2000 data sets use a 14-day period. A

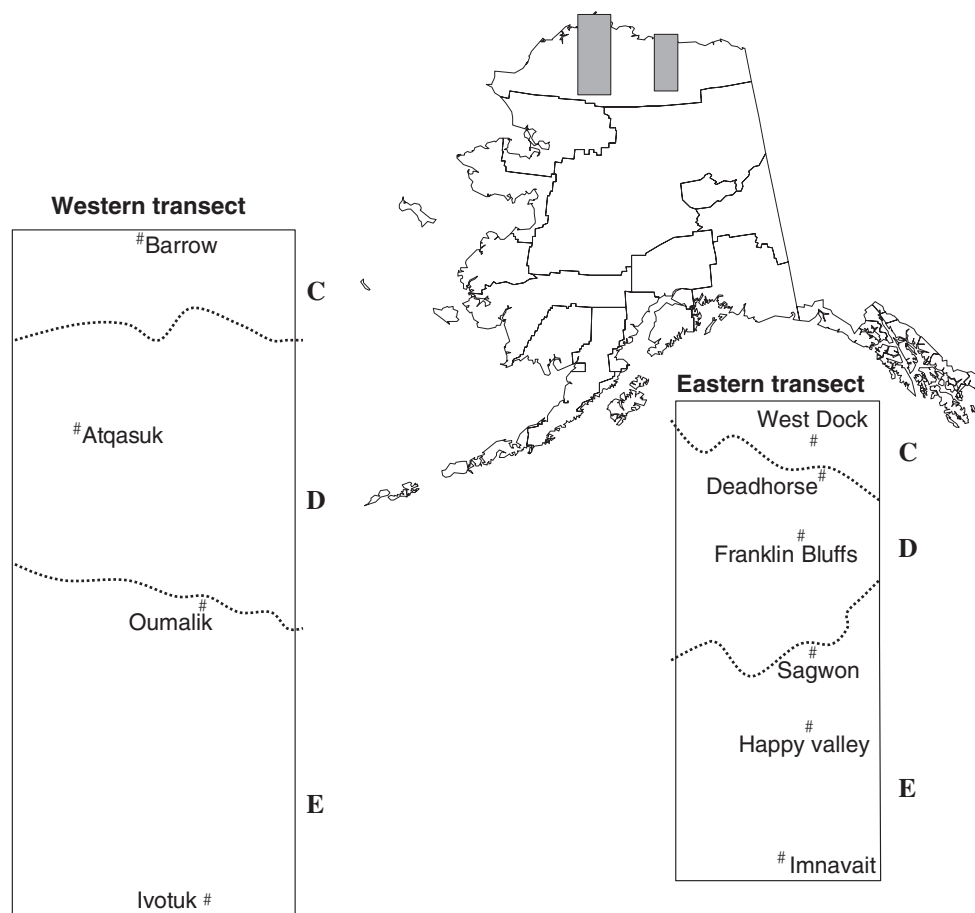


Fig. 1 Location of the study sites with respect to bioclimate subzones and vegetation transects. The dotted lines show the boundaries of bioclimate subzones, C, prostrate dwarf shrub subzone (north); D, erect dwarf shrub subzone (middle); and E, low shrub subzone (south). The solid polygons are the boundaries of transects used in our study. Black points represent the study sites.

cross-calibration between the two sensors was performed by the USGS Biological Resources Division to correct the signal degradation (Markon, 1999). Two additional AVHRR data sets, a newly calibrated and corrected 1990–2000 8 km 15-day composited NDVI time series and a 1992–1993 1 km 10-day NDVI composite datasets were used to normalize our time series. A ratio of composite days between the NOAA-11 and NOAA-14 data sets was introduced to make the data between 1991–1994 and 1995–2000 more comparable in terms of time-integrated values.

Two NDVI indices, Peak-NDVI and TI-NDVI were developed to represent annual characteristics of vegetation greenness. Peak-NDVI is the maximum measurable NDVI recorded during the year and is associated with the peak of greenness during the growing season. In our study area, it occurs in late-July to early-August.

TI-NDVI is the cumulative value of NDVI recorded during each growing season; therefore, this index reflects accumulated vegetation activity within a year. The grow-

ing season was defined as the period when the NDVI time series curve was above a value of 0.09 (Goward *et al.*, 1991; Jia *et al.*, 2002). ArcInfo software was used to calculate mean annual values and temporal variation (standard deviation) of Peak-NDVI and TI-NDVI for the period from 1991 to 2000. The means and variation datasets were spatially summarized for 0.1° latitude intervals along both western and eastern transects and for the three bioclimate subzones along each transect based on a bioclimate map (Walker, 2000). Ocean and inland water bodies greater than 1 km² (or one pixel) were masked in the calculations, so that only terrestrial NDVI pixels were considered in subsequent analysis.

Length of growing season

A phenological NDVI index, length of growing season, was also derived from NDVI time series for each year. Length of growing season is the total number of days in the growing season for each year. The spatial data sets

Table 1 Summary of characteristics for three bioclimate subzones

Features	Subzone C	Subzone D	Subzone E	Reference
Location in Alaska	North coast	Coastal plain and northern foothills	Foothills of the Brooks Range	*
Vegetation types	MNT, wet tundra	MNT, sandy tundra	MAT, shrub tundra	*
Plant functional types	Prostrate dwarf shrub, moss, graminoids	Graminoids, erect dwarf shrub, moss	Low shrub, Tussock-graminoids	*
Sites in Alaska	Barrow, West Dock, Howe Island	Atqasuk, Oumalik, Deadhorse, West Kugaruk, Franklin Bluffs, Sagwon	Oumalik, Ivotuk, Umiat, Sagwon, Toolik	This study
July air temperature (°C)	5–7	7–9	9–12	†
Summer warmth index (°C)	10.8 ± 1.6	24.6 ± 1.7	29.5 ± 0.83	This study
Total phytomass (g/m ²)	341.3 ± 81.2	482.0 ± 37.9	1049.7 ± 231.0	This study
Vegetation coverage (%)	5–50	50–80	80–100	†
Leaf area index (m ² /m ²)	0.68 ± 0.23	0.92 ± 0.15	1.65 ± 0.39	This study
Shrub cover (%)	12.5 ± 3.5	29.8 ± 5.1	57.0 ± 7.9	This study
Moss cover (%)	37.6 ± 10.7	36.3 ± 5.8	22.6 ± 6.7	This study
Vegetation height (cm)	5–10	10–40	20–80	†

*Walker (2000).

†Walker *et al.* (2003a).

MNT, moist nonacidic tundra; MAT, moist acidic tundra.

of length of growing season were calculated by accumulating the days within the seasonal NDVI curves above a threshold value (0.09). Decadal mean values and temporal variation (standard deviation) of the length of growing season were calculated, and the mean and variance datasets were then summarized for 0.1° latitudinal intervals and for the three bioclimate subzones along each transect, using the same method as for Peak-NDVI and TI-NDVI.

Fractional land cover

The land cover features within the study areas are highly heterogeneous, with different tundra vegetation types and abundance of water bodies along the latitudinal gradients. These various land cover features respond to climate differently and contribute to the spatial pattern of NDVI dynamics. Fractional land cover was spatially summarized with 0.1° latitude intervals along both transects based on an Arctic Slope land cover map produced from a mosaic of Landsat Multispectral Scanner (MSS) images at 100 m spatial resolution (Muller *et al.*, 1999). Among its original nine classes, only the fractional cover of dominant types including wet tundra, moist nonacidic tundra (MNT), moist acidic tundra (MAT), sandy tundra, shrub tundra, and water bodies were calculated for subsequent analysis. Ocean pixels were masked so that only inland water was included in the fractional cover. Sandy tundra was only found along the western transect, therefore, five types were summarized in the east compared with six in the west.

Interpretation of biomass from NDVI

Aboveground plant biomass was measured during peak growing season at 17 sites widely distributed throughout the study areas to represent the different subzones and major vegetation types. For each site six to ten random 20 cm × 50 cm clip-harvest plots were selected within a 100 m × 100 m grid to represent plant biomass for the grid with homogenous vegetation; the biomass samples were then dried to constant weight (Walker *et al.*, 2003b; Riedel *et al.*, 2005). Supporting analyses demonstrate that six to ten 20 cm × 50 cm samples are adequate for characterizing the mean and standard deviation of total aboveground green biomass for the 100 m × 100 m grids (Riedel *et al.*, 2005). TI-NDVI values were summarized from 3 × 3 AVHRR pixel blocks around each biomass sampling site. The field scale biomass data were used in a regression analysis with the NDVI values averaged from the nine pixels centered on each site. The best regression model was selected to determine aboveground plant biomass from NDVI. Our biomass sample sites were situated within relatively homogeneous vegetation areas that are large enough to cover 3 × 3 AVHRR pixels. To ensure the match of scale between the biomass sampling (within 100 × 100 m²) and AVHRR pixels (1 km²), we used aerial photos and Landsat-7-derived NDVI (30 m resolution) to assess the spatial variance within each correspondent 3 × 3 AVHRR pixel block. Histograms of the Landsat-NDVI distribution and the spatial variance for each site were constructed.

Regression modeling between NDVI and SWI

Monthly mean air temperature data time series from NOAA and LAII meteorological stations in the region were used to analyze the temporal–spatial relationships between NDVI and summer warmth index (SWI). SWI, the sum of mean monthly air temperatures greater than 0 °C, was calculated from 1991 to 2000 (whenever data were available) for each of the stations and compared with the NDVI interannual series. Regressions were performed spatially by using the time series of all the stations and temporally for each station between SWI and TI-NDVI or Peak-NDVI.

Results and discussion*Fractional land cover*

There were six dominant land cover types along the western transect: wet tundra, MNT, MAT, shrub tundra, sandy tundra, and water (mainly thaw lakes). All the

types but sandy tundra were also dominant on the eastern transect (Table 2; Fig. 2). About 34.8% of the western transect was covered by MAT, 18.9% by shrub tundra, while the other four types almost equally covered the remaining area. Large numbers of thaw lakes in subzone C made wet tundra and water cover over 55.4% of the total area of that subzone. Zonal vegetation was replaced by sandy tundra in about 19.6% of subzone D, making it unique compared with the east. On the eastern transect MNT became the predominant type with 40.1% of the total cover and 58.5% of subzone D, while MAT and shrub tundra occupied 70.6% of subzone E. Compared with the western transect, there is less thaw lake area (5.5% vs. 10.2%) and no sandy tundra. Each land cover type had its specific areas of dominant cover along the latitudinal gradients. For example, shrub tundra and MAT had large fractional cover in the southern latitudes and declined northwards, while wet tundra and water bodies had large fractional cover in the north coastal areas and declined southwards. Sandy tundra was distributed strictly in

Table 2 Fractional land cover summarized by transects and bioclimate subzones

Area	Wet tundra	MNT	MAT	Shrub tundra	Sandy tundra	Water
<i>Western transect</i>						
Subzone C	0.296	0.393	0.015	0.001	0.010	0.258
Subzone D	0.223	0.151	0.220	0.037	0.190	0.175
Subzone E	0.005	0.051	0.545	0.363	0.000	0.036
Mean	0.129	0.123	0.348	0.189	0.081	0.102
<i>Eastern transect</i>						
Subzone C	0.386	0.364	0.004	0.004	0.000	0.191
Subzone D	0.218	0.585	0.048	0.029	0.000	0.072
Subzone E	0.025	0.236	0.468	0.238	0.000	0.018
Mean	0.137	0.401	0.237	0.127	0.000	0.055

MNT, moist nonacidic tundra; MAT, moist acidic tundra.

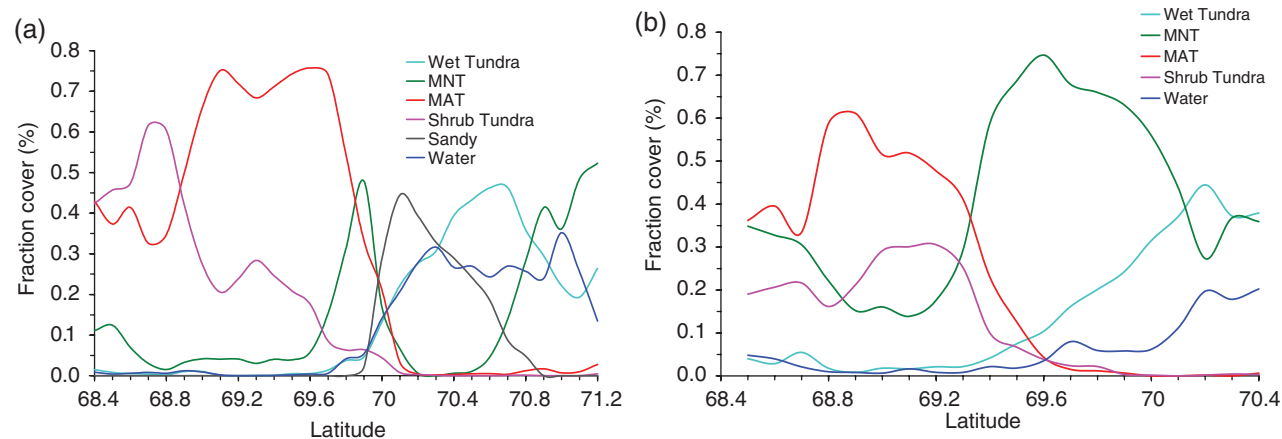


Fig. 2 Fractional covers of tundra vegetation along the latitudinal gradients for each transect. The fractional covers were summarized for 0.1° latitude intervals over a vegetation map of the (a) Western Transect and (b) Eastern Transect modified from Muller *et al.* (1999).

latitudes between 70.9°N and 70.3°N on the western transect (Table 2).

Spatial gradients of NDVI

As expected, both Peak-NDVI and TI-NDVI for the two transects exhibited the direct response of vegetation to the latitudinal gradient of air temperature (Fig. 3). Both

indices increased systematically with decreasing latitude along the transects. There was a relatively low and flat NDVI between 71.2°N and 70.4°N, constant increase from 70.4°N to 69.4°N, high and flat values from 69.4°N to 69.1°N, and a slight drop around 69.4–68.4°N. The steepest spatial increases of Peak-NDVI and TI-NDVI were observed from 70.3°N to 69.5°N, which corresponded to subzone D and the transition between

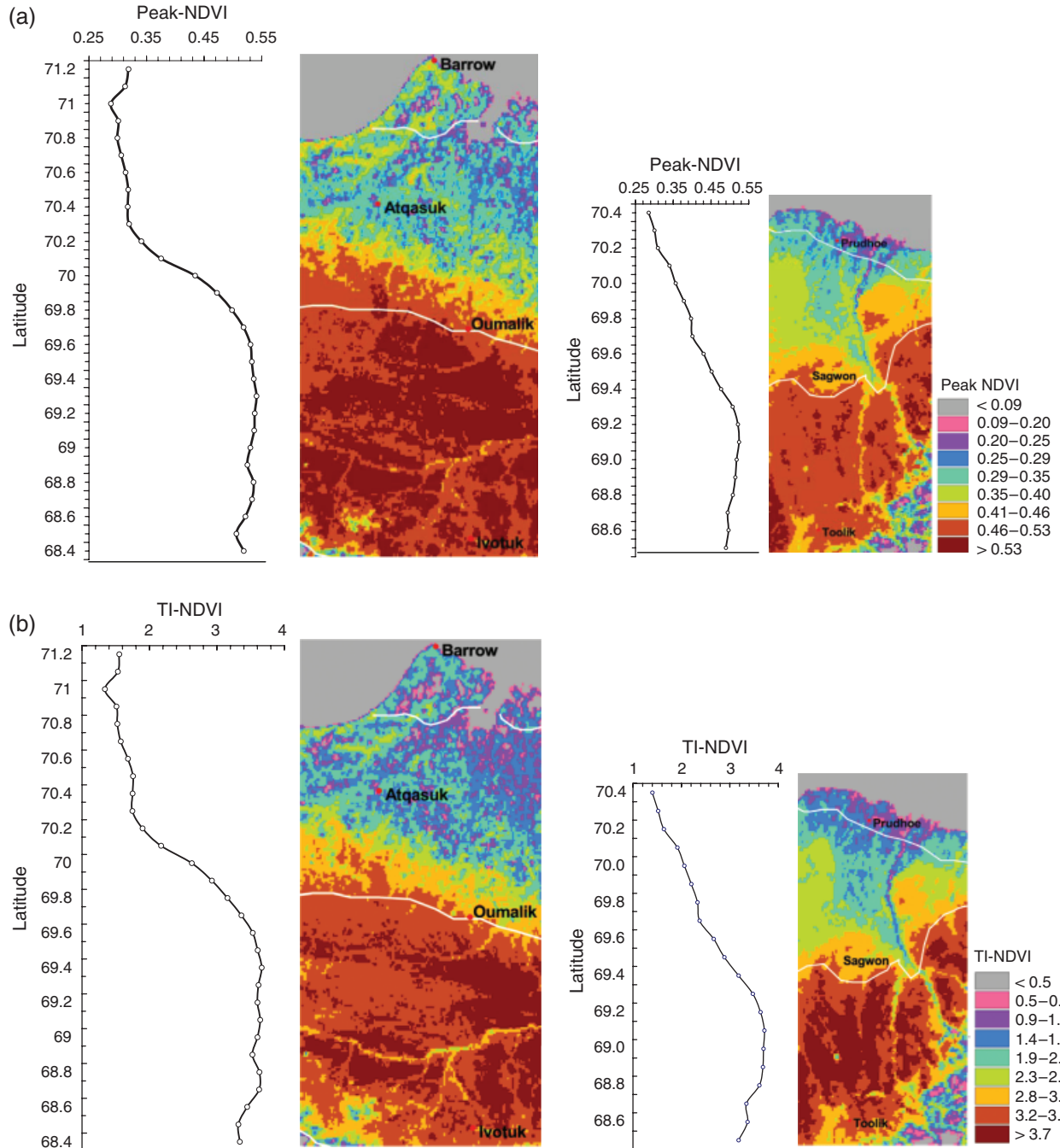


Fig. 3 Spatial patterns of decadal mean (a) Peak-NDVI and (b) TI-NDVI shown as images and summarized for 0.1° latitude intervals along latitudinal gradients for each transect.

subzones D and E (or between MNT and MAT). However, there were some exceptions from the systematic latitudinal patterns. On the western transect, the lowest point for both NDVI indices (0.28 for Peak-NDVI and 1.34 for TI-NDVI) was observed around 71°N, and only slight changes of Peak-NDVI and TI-NDVI occurred between 70.9°N and 70.3°N. Those patterns were most likely caused by their unique land covers. There was 35.2% of water cover at 71°N, the highest point of fractional water cover along the transect. At the sub-pixel scale, the high proportion of water in the spectral mixture of the 1 km AVHRR pixels certainly lowered NDVI values (a pure water pixel has a negative NDVI). Therefore, low NDVI values did not necessarily demonstrate low vegetation productivity; instead, they were likely the result of low coverage of vegetated areas. The area between 70.9°N and 70.3°N is characterized by the extension of sandy tundra (22.5%) that grows on a Quaternary sand sea around Atqasuk. As azonal vegetation, sandy tundra is relatively insensitive to zonal environmental gradients (Walker *et al.*, 2003a). Meanwhile, water covered 20.7–31.4% of this area, which definitely contributed to the insensitivity of NDVI along the environmental gradients (Table 2).

The spatial patterns of decadal mean NDVI indices along latitudinal gradients can be explained in part by the seasonal and latitudinal trends in summer air temperature and the differential responses of different vegetation types. In the Arctic, latitudinal variations in summer air temperature cause concomitant variations in the durations of snow and ice cover, primary production, species composition, and biogeochemical cycling (Oechel & Billings, 1992; Oberbauer *et al.*, 1998). The ambient SWI values were on average 10.8, 24.6, and 29.5°C for bioclimate subzones C, D, and E, respectively. These latitudinal summer warmth regimes are the predominant driving forces for the geographical differences of various environmental factors in this warmth-limited environment. For example, soil organic layer thickness varied from 4.3 cm in subzone C and 8.3 cm in subzone D to 17.4 cm in subzone E (Walker *et al.*, 2003b). The vegetation types in the southern subzones had greater aboveground plant biomass, vegetation cover, leaf area index, vegetation height, and fractional shrub cover than the vegetation types in the northern subzones (Table 1), which explains the north-south NDVI spatial gradients. The latitudinal gradients of length of growing season (Fig. 4a) also followed patterns of both Peak-NDVI and TI-NDVI.

Interannual NDVI variance

Unlike the mean values of NDVI, the spatial patterns of NDVI interannual variance were far more heteroge-

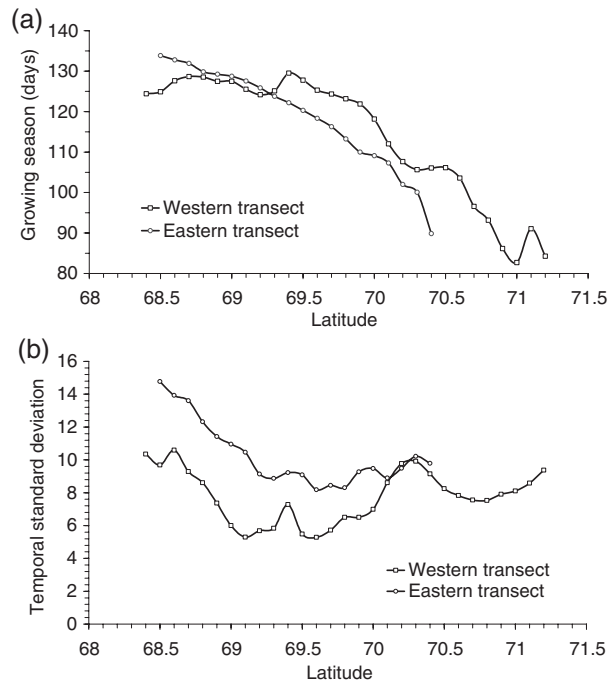


Fig. 4 Spatial patterns of decadal (a) mean values and (b) interannual standard deviations in NDVI-derived length of growing season as summarized for 0.1° latitude intervals along latitudinal gradients for each transect.

neous and complex (Fig. 5). Peak-NDVI exhibited high interannual variance throughout subzones C and D, with the exception of the sandy tundra area along the western transect. Peak-NDVI had some high values of interannual variances in the more southern latitudes; however, there was a general trend of greater Peak-NDVI variance with increasing latitude along both transects. TI-NDVI variance, however, showed a different latitudinal pattern: greater variance occurred in the lower latitudes, associated with subzone E where shrub tundra and MAT dominated, and decreased northwards. Relatively greater temporal variances in both Peak-NDVI and TI-NDVI were also detected near the boundary between subzones C and D, particularly for the western transect.

Fractional land cover possibly contributed to the spatial heterogeneity of NDVI variance. The latitudinal gradient of Peak-NDVI variance roughly followed the gradient of wet tundra, while the TI-NDVI variance fitted well with the gradient of shrub tundra (Fig. 2, Tables 2, and 3). Maximum Peak-NDVI variance occurred at two latitudes, 71.2°N and 69.9°N along the western transect and 69.8°N along the eastern transect where the peak MNT fractional cover (47.9%, 52.3% and 74.7%, respectively, for the west and east) was located. The maximum of TI-NDVI variance occurred at 68.7°N along the western transect and 68.8°N along the eastern

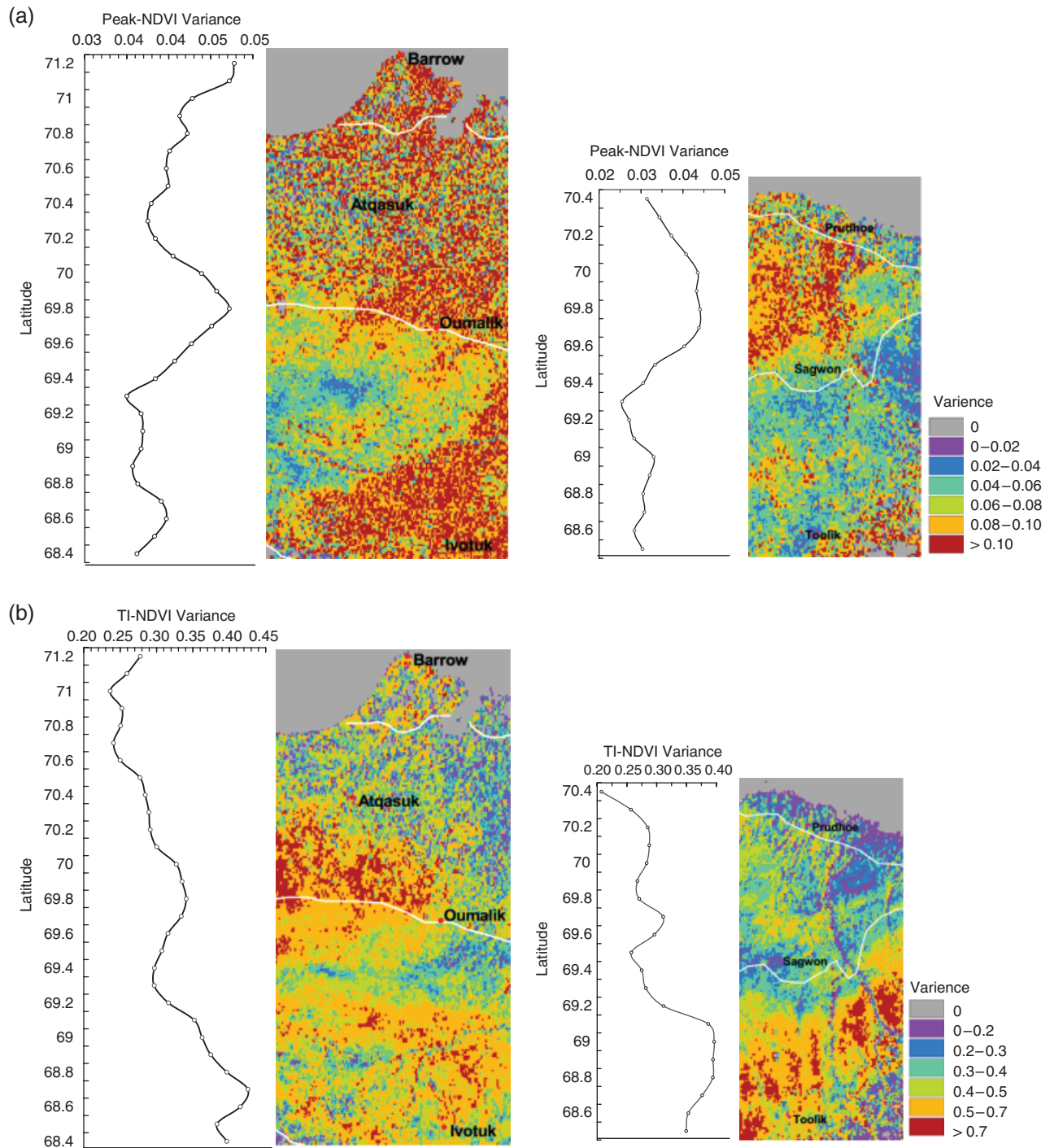


Fig. 5 Spatial patterns of decadal temporal variation in (a) peak-normalized difference vegetation index (NDVI) and (b) time-integrated (TI)-NDVI shown as images and as summarized for 0.1° latitude intervals along latitudinal gradients for each transect.

transect corresponding to the peak of shrub cover (61.6%) and MAT cover (75.7%), respectively (Table 2). These different spatial patterns of interannual variance between Peak-NDVI and TI-NDVI may also reflect the different aspects of vegetation phenology they repre-

sent. Peak-NDVI indicates maximum NDVI within a year and its interannual variance reflects dynamics of the photosynthesizing portion of the annual peak vegetation biomass. MNT and wet tundra contain a higher percentage of graminoids and annuals and less shrubs

Table 3 Correlations among NDVI, NDVI variances, length of growing season, and fractional land cover.

Variables	<i>r</i>	<i>P</i>	<i>N</i>
Peak-NDVI variance vs. Peak-NDVI	-0.712	< 0.001	49
Peak-NDVI variance vs. TI-NDVI	-0.768	< 0.001	49
Peak-NDVI variance vs. TI-NDVI variance	-0.609	< 0.001	49
Peak-NDVI variance vs. length of growing season	-0.826	< 0.001	49
Peak-NDVI variance vs. length of growing season variance	-0.234	0.105	49
Peak-NDVI variance vs. WT	0.589	< 0.001	49
Peak-NDVI variance vs. MNT	0.136	0.350	49
Peak-NDVI variance vs. MAT	-0.597	< 0.001	49
Peak-NDVI variance vs. shrub tundra	-0.461	0.001	49
Peak-NDVI variance vs. sandy tundra	0.224	0.121	49
TI-NDVI variance vs. Peak-NDVI	0.725	< 0.001	49
TI-NDVI variance vs. Peak-NDVI variance	-0.609	< 0.001	49
TI-NDVI variance vs. TI-NDVI	0.767	< 0.001	49
TI-NDVI variance vs. length of growing season	0.825	< 0.001	49
TI-NDVI variance vs. length of growing season variance	0.579	< 0.001	49
TI-NDVI variance vs. WT	-0.709	< 0.001	49
TI-NDVI variance vs. MNT	-0.120	0.413	49
TI-NDVI variance vs. MAT	0.528	< 0.001	49
TI-NDVI variance vs. shrub tundra	0.691	< 0.001	49
TI-NDVI variance vs. sandy tundra	-0.312	0.029	49

Two-tailed Pearson's correlation analysis was performed on the 0.1° latitude summary of the variables for both transects. Key relationships are in bold.

TI-NDVI, time-integrated-normalized difference vegetation index; NDVI, normalized difference vegetation index; MNT, moist nonacidic tundra; MAT, moist acidic tundra; WT, wet tundra.

compared with MAT and shrub tundra (Walker *et al.*, 1998). This may have led to higher interannual changes of peak green biomass, because graminoids and annuals are more sensitive to temporal environmental fluctuation, while the woody component varies little from year to year and makes little contribution to NDVI variance (Wookey *et al.*, 1993; Walker *et al.*, 1998; Walker, 2000). TI-NDVI, on the other hand, is an integrated index of NDVI values throughout a growing season, and therefore, its interannual variance reflects the entire growing season. As a longer growing season contributes to TI-NDVI in the south (subzone E) compared with the north, there is the potential for greater variance in this index at the more southern locations. This is especially true considering the high temporal variance of the length of growing season in subzone E (Fig. 4). Another interesting pattern is that there were relatively low temporal variances for both NDVI indices between 70.9°N and 70.3°N where sandy tundra and water together covered approximately half of the landscape. The vegetation greenness of sandy tundra was not as sensitive to environmental dynamics as zonal vegetation, and the NDVI of water essentially does not change temporally (Goward *et al.*, 1991). The high fractional cover of sandy tundra and water in AVHRR pixels therefore buffered interannual variance of NDVI.

As mentioned above, the general trends and spatial heterogeneity of NDVI variances can be explained in part by interannual variances in the length of growing season, (i.e. NDVI increases in warm years may result from lengthening of the growing season caused by earlier onset of growth and/or delayed senescence), and large temporal NDVI variances in certain areas may be associated with large variances in length of growing season, as well. This was supported by the latitudinal patterns of temporal variances in length of growing season for each transect (Fig. 4b). For example, the great variances in length of growing season near the southern end of the transects clearly corresponded to great variances in TI-NDVI.

Other possible explanations for the heterogeneity in vegetation dynamics are soil parent material and patterned-ground formations because of freeze–thaw processes. Sandy soil material in most of subzone D along the western transect supports some of the smallest decadal changes in both NDVI indices. Also, nonsorted circles (also known as frost boils) exist widely throughout the Arctic Slope, and the size and density of frost boils tend to increase from south to north. The abundance of frost boils may negatively affect the response of landscape and regional scale vegetation to climate fluctuations (Walker *et al.*, 2003b), because of freeze–

thaw disturbance limitations, and therefore, may have buffered changes of NDVI and biomass to a greater extent in certain areas where they predominate on the landscape.

The high temporal variance of TI-NDVI in the south may be related to an enhancement of shrub growth and a lengthening of the growing season, whereas the high Peak-NDVI variance near the transitional areas in subzones C and D may have reflected the rapid response of vegetation productivity to environmental dynamics and species composition changes (Chapin *et al.*, 1995; Shaver *et al.*, 2001). The relative sensitivity of transition zones has been demonstrated in various biomes such as grassland (Paruelo *et al.*, 1999) and savanna (Scanlon *et al.*, 2002). There was evidence from experiments at the Toolik Lake Long-Term Ecological Research site in northern Alaska (subzone E) showing an increase in shrub growth under warming and control conditions (Chapin *et al.*, 1995; Hobbie & Chapin, 1998), in addition to results from the ITEX which indicated shrub increases circumpolarly (Walker *et al.*, 2004). Sturm *et al.* (2001) reported a substantial increase in shrub abundance in subzone E of the Alaskan Arctic during the past 50 years, which they believe has contributed to increased productivity in some areas. While the abundance of thaw lakes on the coastal plains may delay the spring snowmelt and subsequent warming of soils, increased Peak-NDVI may still be seen in years with high summer temperatures and early snowmelt. Vegetation in the relatively well-drained subzone E is likely to respond to the dynamics of air temperature in the spring more rapidly than the vegetation further north and, therefore, is likely to show a higher cumulative greenness (or TI-NDVI) in warmer years.

Aboveground plant biomass

Annual aboveground plant biomass datasets were calculated by extrapolating observed values obtained from field sites widely located within the region (Figs 6 and 7). Our biomass sample sites were selected at relatively homogeneous vegetation areas, and the standard deviation of Landsat-NDVI within each 3×3 AVHRR pixel block ranges from 0.026 to 0.116 ($n = 11\,436$) (Table 4). The best NDVI–biomass relationship was found between TI-NDVI and aboveground total plant biomass ($r^2 = 0.84$, $P < 0.001$). As a result, the regression equation was used to determine biomass from TI-NDVI for each year. The decadal mean values and interannual variance of biomass were then calculated. As a simulated data layer, biomass showed similar spatial patterns of mean and temporal variances along latitudinal gradients as TI-NDVI. Generally, there was a slight but constant increase of plant biomass from the north coast

towards the Brooks Range along both transects. Steep spatial gradients of biomass were observed from 69.5°N to 70.3°N, which corresponded to the transition between subzones D and E. Biomass was relatively low (220–340 g/m²) and flat from 71.2°N to 70.2°N on the coastal plain, then increased substantially southwards until the boundary between subzones D and E. It was flat and high (630–880 g/m²) in subzone E, with a slight drop at southern edge. Similar to TI-NDVI, the greatest temporal variability in biomass can be found in the southern portion of both transects, which is associated with subzone E, and along the subzones D–E transition. However, compared with TI-NDVI there was relatively flat and low variance in biomass in the coastal areas. The amplitudes of biomass temporal variances were slightly greater than those for NDVI, because of the nonlinear relationship between TI-NDVI and biomass; therefore, in some areas slight change in TI-NDVI reflected more dramatic changes of biomass.

The biomass interpretation was based on one-time biomass measurement from field sites along the gradients, because of the lack of a biomass time series over the last decade for the region. While the mean values were interpreted with confidence considering the high correlation, caution must be taken with the temporal variance of the biomass data layer. Those interpreted values may only demonstrate the general patterns of heterogeneity, and additional time series-based interpretations should be performed whenever data become available.

Effect of summer warmth

Both Peak-NDVI and TI-NDVI showed positive correlations with the SWI for the sites distributed across both transects and the three subzones. When the time-series data from all the sites were used for temporal–spatial regression modeling, SWI explained 70% of the TI-NDVI variance and 58% of the Peak-NDVI variance. These high correlations suggest that the NDVI was largely controlled by cumulative summer temperatures (SWI) at an interannual temporal scale along latitudinal gradients. When the SWI time series for each site were analyzed against the time series of NDVI indices, the correlations were all positive and varied from $r^2 = 0.14$ – 0.44 for Peak-NDVI and $r^2 = 0.17$ – 0.46 for TI-NDVI. The regressions for the entire region reflect both temporal and spatial correlations, and demonstrated that variance in NDVI corresponds to a general pattern of fluctuation and trends of summer temperatures (Fig. 8). During the period of this study, there have been warming-related trends in the Arctic Oscillation mode of atmospheric circulation (Moritz *et al.*, 2002) and a period of cooling following the Mt Pinatubo eruption (Lucht *et al.*, 2002).

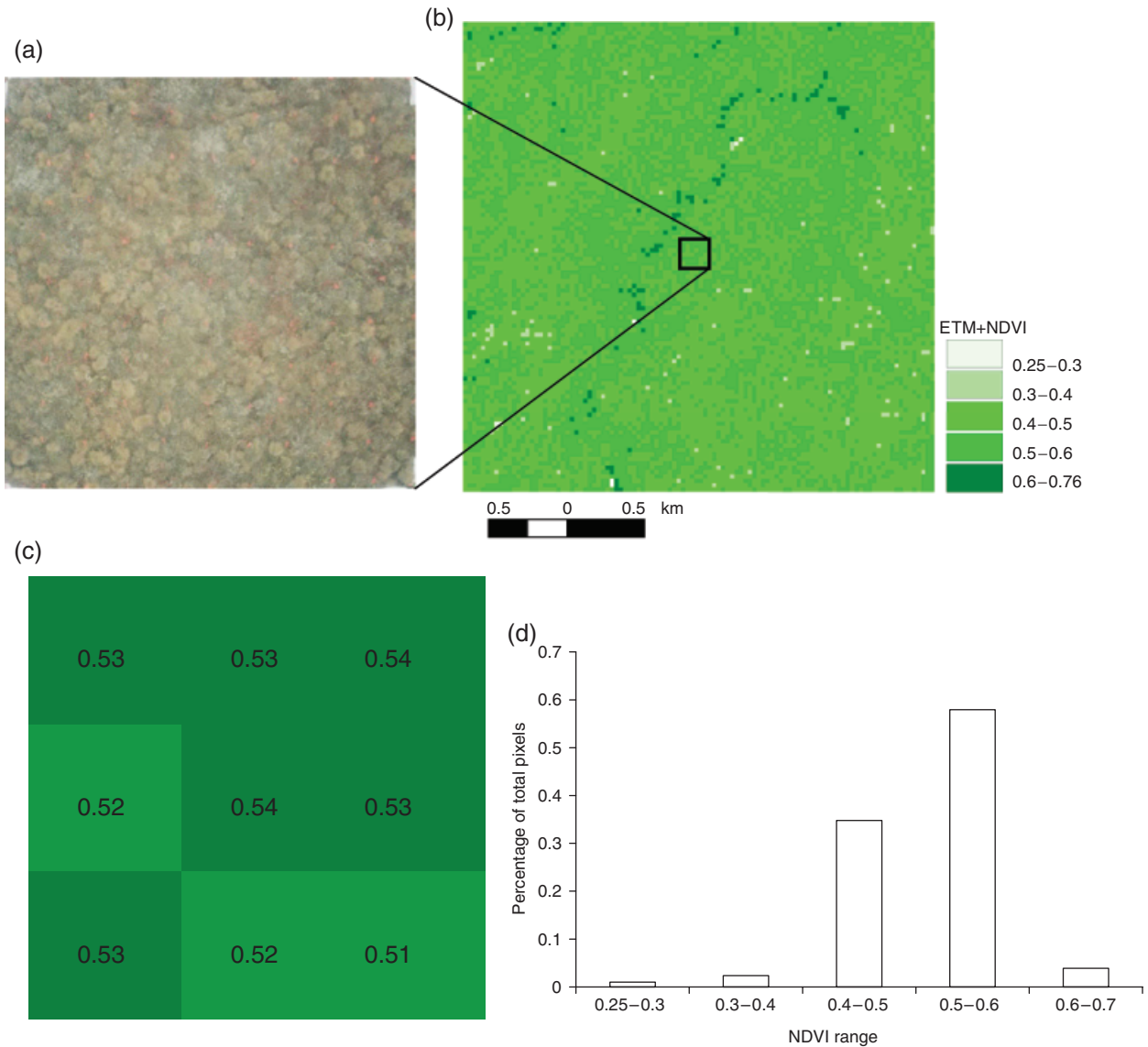


Fig. 6 Hierarchical images of (a) site aerial-photo, (b) Landsat-7-derived normalized difference vegetation index (NDVI), (c) advanced Very High-Resolution Radiometer -derived NDVI, and (d) histograms of the Landsat-NDVI distribution over a 3 km × 3 km sample polygon at Happy Valley, northern Alaska, showing the field sample sites are representative of the 9 km² polygon in term of NDVI.

These temporal climate patterns were reflected by both NDVI indices. Generally, years with greater NDVI values coincide with warm temperatures, and drops in NDVI correspond with cold summers. Reduced cover time and thickness of snow and ice (Groisman *et al.*, 1994) and thaw processes of permafrost (Osterkamp & Romanovsky, 1996) in some areas are direct results of surface warming and have contributed to a longer growing season, which led to greater TI-NDVI and biomass in corresponding areas (Hope *et al.*, 2003; Jia *et al.*, 2003). Warmer springtime temperatures lead to earlier snowmelt and more rapid soil thawing (Hinzman *et al.*, 1998), and the earlier snowmelt in warmer years causes earlier

ecophysiological activity and an overall lengthening of the growing season; a pattern that was apparent from the NDVI-derived metrics (Fig. 4). Warmer and drier soils in warm years are likely to yield higher rates of nutrient mineralization as well (Oechel & Billings, 1992), the latter being critically important for the enhancement of vegetation productivity in the nutrient-limited tundra environment (Shaver *et al.*, 2001).

In summary, the overall interannual variances of Peak-NDVI and TI-NDVI in the region were largely controlled by meso-scale climate dynamics, whereas the spatial heterogeneity of the variances reflected response of different vegetation types, patterned-ground features

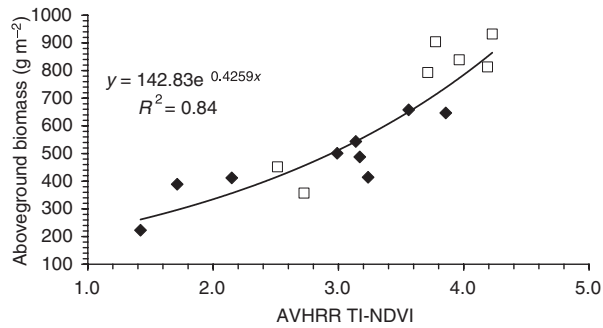


Fig. 7 Regression model between time-integrated-normalized difference vegetation index (TI-NDVI) and total aboveground plant biomass. The biomass values were summarized from six to ten 20 cm × 50 cm clip measurements in each 100 m² field site throughout the region. Diamonds and squares are moist non-acidic tundra (MNT) and moist acidic tundra (MAT) sites, respectively.

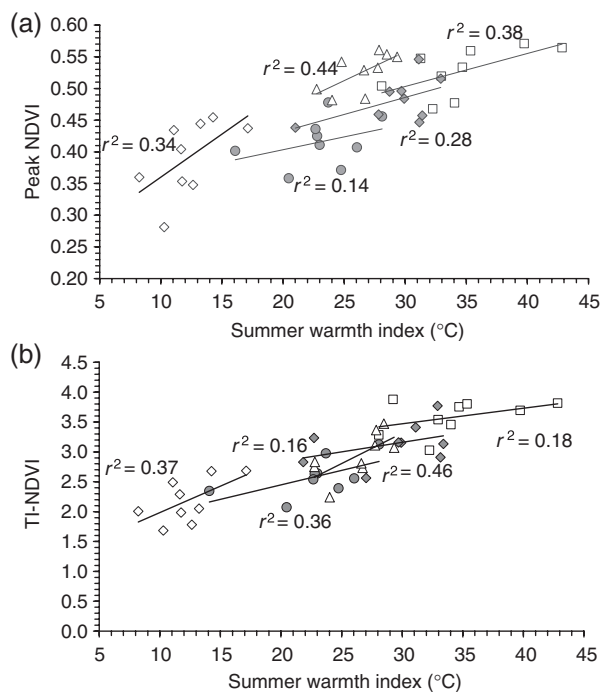


Fig. 8 Temporal-spatial regression models (a) between Peak-normalized difference vegetation index (NDVI) and summer warmth index (SWI) and (b) between time-integrated (TI)-NDVI and SWI based on meteorological records located within the study areas, combined time series with spatial gradients. ◇, Barrow; ●, Prudhoe; ◆, Franklin Bluffs; △, Imnavait, □, Umiat.

and length of growing season to climate fluctuations. In this 10-year time period, the observed NDVI temporal variances are mixed signals of fluctuation and directional change of vegetation greenness. The uncertainties observed with NDVI time series are at global and

Table 4 Statistics of Landsat-7-derived NDVI for each 3 km × 3 km biomass sample site.

Site	Minimum	Maximum	Mean	Standard deviation
West Dock	0.000	0.528	0.242	0.093
Howe Island	0.000	0.369	0.206	0.084
Deadhorse	0.062	0.472	0.256	0.046
Pipeline Crossing	0.093	0.599	0.351	0.062
Oumalik MNT	0.216	0.552	0.382	0.026
Franklin Bluffs	0.107	0.517	0.299	0.037
Pump Station 2	0.147	0.567	0.326	0.045
Sagwon MNT	0.187	0.616	0.385	0.047
Ivotuk MNT	0.156	0.583	0.345	0.043
Barrow	0.000	0.424	0.196	0.116
Atqasuk	0.000	0.483	0.262	0.096
Oumalik MAT	0.061	0.731	0.537	0.036
Sagwon MAT	0.285	0.755	0.523	0.047
Happy Valley	0.297	0.761	0.548	0.039
Ivotuk MAT	0.371	0.734	0.560	0.036

MNT, moist nonacidic tundra; MAT, moist acidic tundra.

The 3 km × 3 km polygons are centered at the 100 m field biomass plots and are spatially related to the 3 × 3 AVHRR pixels used for NDVI-biomass regressions.

regional scales, and are unlikely to affect the spatial patterns of NDVI variances. The locations and vegetation types observed in this study with the greatest temporal NDVI variance could be 'hotspots' for future environmental changes in the region and need more attention for further investigation at finer scales.

Conclusions

The temporal variances of Peak-NDVI and TI-NDVI over the past decade were highly heterogeneous along two latitudinal transects on the Arctic Slope of Alaska. The largest variance in Peak-NDVI occurred in the central part of bioclimate subzone D and was associated with maximum fractional cover of wet tundra and MNT, while the greatest variance in TI-NDVI was observed in the southern part of the latitudinal transects and was associated with maximum shrub tundra/MAT fractional cover. Relatively high temporal NDVI variances were also found around several transitions along the gradients. Existence of azonal vegetation (i.e. sandy tundra) and water bodies lowered the temporal NDVI variances in corresponding areas because of their insensitivity to environmental dynamics. Although the regional temporal variances of NDVI from 1991 to 2000 were mostly driven by meso-scale climate dynamics, the spatial heterogeneity mostly reflected responses of different tundra vegetation types to climate along the latitudinal gradients, controlled by fractional land cover

in a given pixel. The relationship between NDVI and biomass was nonlinear; therefore, there was higher amplitude of biomass variance than that for TI-NDVI. Specific factors that may have also contributed to the spatial heterogeneity of NDVI temporal variances are the heterogeneous enhancement of shrub abundance, which is likely because of the distribution of the minimum temperature limit for shrub occurrence (Sturm *et al.*, 2001), the abundance of frost boils on the arctic coastal plain, and the distribution of azonal sandy tundra.

Acknowledgements

This research was funded by the US National Science Foundation (NSF) grants OPP-9908829 and OPP-0120736, and was supported by the BaiRenJiHua of Chinese Academy of Sciences. We thank Carl Markon of the USGS Alaska Geographic Science Office for providing AVHRR data sets. We thank two anonymous referees for their valuable comments on the manuscript.

References

- Anisimov OA, Shiklomanov NI, Nelson FE (1997) Global warming and active-layer thickness: results from transient general circulation models. *Global and Planetary Change*, **15**, 61–77.
- Arft AM, Walker MD, Gurevitch J *et al.* (1999) Response patterns of tundra plant species to experimental warming: a meta-analysis of the International Tundra Experiment. *Ecological Monographs*, **69**, 491–511.
- Bonan GB, Chapin FS III, Thompson SL (1995) Boreal forest and tundra ecosystems as components of the climate system. *Climate Change*, **29**, 145–167.
- Brown J, Hinkel KM, Nelson FE (2000) The circumpolar active layer monitoring (CAVM) program: research designs and initial results. *Polar Geography*, **24**, 165–258.
- Chapin III FS, Eugster W, McFadden JP *et al.* (2000) Summer differences among arctic ecosystems in regional climate forcing. *Journal of Climate*, **13**, 2002–2010.
- Chapin III FS, Shaver GR, Giblin AE *et al.* (1995) Responses of Arctic tundra to experimental and observed changes in climate. *Ecology*, **76**, 694–711.
- Chapin III FS, Sturm M, Serreze MC *et al.* (2005) Role of terrestrial ecosystem changes in Arctic summer warming. *Science*, **310**, 657–660.
- Epstein HE, Beringer J, Gould W *et al.* (2004a) The nature of spatial transitions in arctic ecosystems. *Journal of Biogeography*, **31**, 1917–1933.
- Epstein HE, Calef MP, Walker MD *et al.* (2004b) Detecting changes in arctic plant communities in response to warming over decadal time scales. *Global Change Biology*, **10**, 1325–1334.
- Epstein HE, Walker MD, Chapin III FS *et al.* (2000) A transient, nutrient-based model of arctic plant community response to climatic warming. *Ecological Applications*, **10**, 824–841.
- Goward SN, Markham B, Dye DG (1991) Normalized difference vegetation index measurements from the advanced very high resolution radiometer. *Remote Sensing of Environment*, **35**, 257–277.
- Groisman PY, Karl TR, Knight RW (1994) Observed impact of snow cover on the heat balance and the rise of continental spring temperatures. *Science*, **263**, 198–200.
- Gutman GG (1991) Vegetation index from AVHRR: an update and future prospects. *Remote Sensing of Environment*, **35**, 121–136.
- Hinzman LD, Goering DJ, Kane DL (1998) A distributed thermal model for calculating soil temperature profiles and depth of thaw in permafrost regions. *Journal of Geophysical Research*, **103**, 28975–28991.
- Hobbie SE, Chapin III FS (1998) The response of tundra plant biomass, aboveground production, nitrogen, and CO₂ flux to experimental warming. *Ecology*, **79**, 1526–1544.
- Hope AS, Boynton WL, Stow DA *et al.* (2003) Interannual growth dynamics of vegetation in the Kuparuk River watershed, Alaska based on the Normalized Difference Vegetation. *International Journal of Remote Sensing*, **24**, 1526–1544.
- Jia GJ, Epstein HE, Walker DA (2002) Spatial characteristics of AVHRR-NDVI along latitudinal transects in northern Alaska. *Journal of Vegetation Science*, **13**, 315–326.
- Jia GJ, Epstein HE, Walker DA (2003) Greening of Arctic Alaska, 1981–2001. *Geophysical Research Letters*, **30**, 2067, doi: 10.1029/2003GL018268.
- LAII Science Steering Committee (1997) *Arctic System Science Land–Atmosphere–Ice Interaction LAII, a Plan for Action*. University of Alaska Fairbanks, USA.
- Levis S, Foley JA, Pollard D (1999) Potential high latitude vegetation feedbacks on CO₂-induced climate change. *Geophysical Research Letters*, **26**, 747–750.
- Lucht W, Prentice IC, Myneni RB *et al.* (2002) Climatic control of the high-latitude vegetation greening trend and Pinatubo effect. *Science*, **296**, 1687–1689.
- Markon CJ (1999) Characteristics of the Alaskan 1 km advanced very high resolution radiometer data sets used for analysis of vegetation biophysical properties. USGS Open File Report 99-088.
- Moritz RE, Bitz CM, Steig EJ (2002) Dynamics of recent climate change in the Arctic. *Science*, **297**, 1497–1502.
- Muller SV, Racoviteanu AE, Walker DA (1999) Landsat MSS-derived land-cover map of northern Alaska: extrapolation methods and a comparison with photo-interpreted and AVHRR-derived maps. *International Journal of Remote Sensing*, **20**, 2921–2946.
- Oberbauer SF, Starr G, Pop EW (1998) Effects of extended growing season and soil warming on carbon dioxide and methane exchange of tussock tundra in Alaska. *Journal of Geophysical Research*, **103**, 29075–29082.
- Oechel WC, Billings WD (1992) Effects of global change on the carbon balance of arctic plants and ecosystems. In: *Arctic Ecosystems in a Changing Climate* (eds Chapin FS, Jeffries RL, Reynolds JF, Shaver GR, Svoboda J), pp. 139–168. Academic Press, San Diego, USA.
- Oechel WC, Vourlitis GL, Hastings SJ *et al.* (2000) Acclimation of ecosystem CO₂ exchange in the Alaskan Arctic in response to decadal climate warming. *Nature*, **406**, 978–981.
- Osterkamp TE, Romanovsky VE (1996) Characteristics of changing permafrost temperatures in the Alaskan arctic, USA. *Arctic and Alpine Research*, **28**, 267–273.

- Paruelo JM, Lauenroth WK, Burke IC *et al.* (1999) Grassland precipitation-use efficiency varies across a resource gradient. *Ecosystems*, **2**, 64–68.
- Riedel SM, Epstein HE, Walker DA *et al.* (2005) Spatial and temporal heterogeneity of LAI, NDVI and aboveground net primary production for four tundra types in northern Alaska. *Arctic, Antarctic and Alpine Research*, **37**, 35–42.
- Scanlon TM, Albertson JD, Caylor KK *et al.* (2002) Determining land surface fractional cover from NDVI and rainfall time series for a savanna ecosystem. *Remote Sensing of Environment*, **82**, 376–388.
- Serreze MC, Walsh JE, Chapin III FS *et al.* (2000) Observational evidence of recent change in the northern high-latitude environment. *Climatic Change*, **46**, 159–207.
- Shaver GR, Bret-Harte MS, Jones MH *et al.* (2001) Species composition interacts with fertilizer to control long-term change in tundra productivity. *Ecology*, **82**, 3163–3181.
- Sturm M, Racine C, Tape K (2001) Increasing shrub abundance in the Arctic. *Nature*, **411**, 546–547.
- Walker DA (2000) Hierarchical subdivision of arctic tundra based on vegetation response to climate, parent material, and topography. *Global Change Biology*, **6**, 19–34.
- Walker DA, Auerbach NA, Bockheim JG *et al.* (1998) Energy and trace-gas fluxes across a soil pH boundary in the Arctic. *Nature*, **394**, 469–472.
- Walker DA, Epstein HE, Gould WA *et al.* (2004) Frost-boil ecosystems: complex interactions between landforms, soils, vegetation and climate. *Permafrost and Periglacial Processes*, **15**, 171–188.
- Walker DA, Epstein HE, Jia GJ *et al.* (2003a) Phytomass, LAI, and NDVI in northern Alaska: relationships to summer warmth, soil pH, plant functional types and extrapolation to the circumpolar Arctic. *Journal of Geophysical Research*, **108**, 8169.
- Walker DA, Jia GJ, Epstein HE *et al.* (2003b) Vegetation–soil–thaw–depth relationships along a low arctic bioclimate gradient, Alaska: synthesis of information from the ATLAS studies. *Permafrost and Periglacial Processes*, **14**, 103–123.
- Wookey PA, Parsons AN, Welker JM *et al.* (1993) Comparative responses of phenology and reproductive development to simulated environmental changes in sub-arctic and high arctic plants. *Oikos*, **67**, 490–502.
- Zhou L, Tucker CJ, Kaufmann RK *et al.* (2001) Variations in northern vegetation activity inferred from satellite data of vegetation index during 1981 to 1999. *Journal of Geophysical Research*, **106**, 20069–20083.